

$\text{cm}^{-3}$ ) assuming one water molecule per unit cell. It may be that the water position is filled in fresh crystals, but only half-filled in the crystal which was exposed to an atmosphere of 50% humidity during x-ray exposure. The zeolitic channels through which these water molecules may move are apparent in Figure 5, parallel to  $c$ , the line of view. This is plausible and, if it is correct, the calculated density would be  $1.655 (2) \text{ g cm}^{-3}$ , somewhat closer to the value observed by flotation.

The water oxygen atom is  $3.18 \text{ \AA}$  from O(67), the oxygen atom with the smallest thermal parameter in its perchlorate group, which otherwise has large thermal parameters (Table I) and Cl-O distances which are severely foreshortened (Table III). Together, these observations indicate the presence of a hydrogen bond between O(67) and O(69). This contact can be seen in Figure 5, the stereoview of the crystal structure. The contact distance O(69)-C(53) is also short,  $3.27 \text{ \AA}$ , and O(69)-H(53) is calculated to be  $2.4 \text{ \AA}$ .

**Acknowledgment.** This work was supported by the National Institutes of Health (Grant No. GM-18813-04). We are indebted to Professor John W. Gilje for valuable discussions of the bonding in the ligand, and to the University of Hawaii Computing Center.

**Supplementary Material Available:** observed and calculated structure factors (20 pages). Ordering information is given on any current masthead page.

## References and Notes

- (1) P. E. Riley and K. Seff, *Inorg. Chem.*, **11**, 2993 (1972).
- (2) T. Ottersen, L. G. Warner, and K. Seff, *Inorg. Chem.*, **13**, 1904 (1974).
- (3) L. G. Warner, T. Ottersen, and K. Seff, *Inorg. Chem.*, **13**, 2819 (1974).
- (4) L. G. Warner, T. Ottersen, and K. Seff, *Inorg. Chem.*, **13**, 2529 (1974).
- (5) L. G. Warner, M. M. Kadooka, and K. Seff, *Inorg. Chem.*, **14**, 1773 (1975).
- (6) J. A. Bertrand and J. L. Breece, *Inorg. Chim. Acta*, **8**, 267 (1974).
- (7) J. A. Thich, D. Mastropaolo, J. Potenza, and H. J. Schugar, *J. Am. Chem. Soc.*, **96**, 726 (1974).
- (8) C.-I. Bränden, *Acta Chem. Scand.*, **21**, 1000 (1967).
- (9) M. M. Kadooka, E. Hilti, L. G. Warner, and K. Seff, *Inorg. Chem.*, **15**, 1186 (1976).

- (10) M. M. Kadooka, L. G. Warner, and K. Seff, *Inorg. Chem.*, **15**, 812 (1976).
- (11) N. V. Raghavan and K. Seff, *Acta Crystallogr., Sect. B*, in press, and references cited therein.
- (12) M. M. Kadooka, L. G. Warner, and K. Seff, *J. Chem. Soc., Chem. Commun.*, 990 (1975).
- (13) W. Byers, G. Curzon, K. Garbett, B. E. Speyer, S. N. Young, and R. J. P. Williams, *Biochim. Biophys. Acta*, **310**, 38 (1973).
- (14) D. A. Baldwin, A. B. P. Lever, and R. V. Parish, *Inorg. Chem.*, **8**, 107 (1969), and references cited therein.
- (15) K. G. Allum, J. A. Creighton, J. H. S. Green, G. J. Minkoff, and L. J. S. Prince, *Spectrochim. Acta, Part A*, **24**, 927 (1968).
- (16) F. R. Dollish, W. G. Fateley, and F. F. Bentley, "Characteristic Raman Frequencies of Organic Compounds", Wiley, New York, N.Y., 1974, p 49.
- (17) W. M. Moreau and K. Weiss, *J. Am. Chem. Soc.*, **88**, 204 (1966).
- (18) B. Nelander, *Spectrochim. Acta, Part A*, **29**, 859 (1973), and references cited therein.
- (19) D. B. Boyd, *Int. J. Quantum. Chem.: Quantum Biol. Symp.*, No. 1, 13 (1974).
- (20) G. Bergson, G. Claesson, and L. Schotte, *Acta Chem. Scand.*, **16**, 1159 (1962).
- (21) R. Malkin and B. G. Malmstrom, *Adv. Enzymol.*, **33**, 177 (1970).
- (22) W. R. Busing and H. A. Levy, *Acta Crystallogr.*, **10**, 180 (1957).
- (23) T. Dahl, Computer Program ABSCO, Chemistry Department, University of Oslo, modified by T. Ottersen, 1973.
- (24) T. Ottersen, Computer Program LP-73, University of Hawaii, 1973.
- (25) C. R. Hubbard, C. O. Quicksall, and R. A. Jacobson, "ALFF, Ames Laboratory Fast Fourier," Iowa State University, 1971.
- (26) K. Seff, Computer Program HFIND, University of Hawaii, 1971.
- (27) M. R. Churchill, *Inorg. Chem.*, **12**, 1213 (1973).
- (28) J. A. Ibers, NUCLS, full-matrix least squares, Northwestern University, Evanston, Illinois, based on ORFLS, by W. R. Busing and H. A. Levy.
- (29) P. A. Doyle and P. S. Turner, *Acta Crystallogr., Sect. A*, **24**, 390 (1968).
- (30) D. T. Cromer, *Acta Crystallogr.*, **18**, 17 (1965).
- (31) R. F. Stewart, E. R. Davidson, and W. T. Simpson, *J. Chem. Phys.*, **42**, 3175 (1965).
- (32) C. K. Johnson, "ORTEP", Oak Ridge National Laboratory, Oak Ridge, Tenn., 1965, Report ORNL-3794.
- (33) T. Ottersen, L. G. Warner, and K. Seff, *Acta Crystallogr., Sect. B*, **29**, 2954 (1973).
- (34) P. T. Buerkens, J. A. Cras, J. H. Noordik, and A. M. Spruijt, *J. Cryst. Mol. Struct.*, **1**, 93 (1971).
- (35) F. Bernardi, I. G. Csizmadia, A. Mangini, H. B. Schlegel, M. H. Whangbo, and S. Wolfe, *J. Am. Chem. Soc.*, **97**, 2209 (1975).
- (36) H. E. Van Wart, L. L. Shipman, and H. A. Scheraga, *J. Phys. Chem.*, **79**, 1436 (1975).
- (37) S. Wolfe, A. Rauk, L. M. Tel, and I. G. Csizmadia, *J. Chem. Soc. B*, 136 (1971).
- (38) R. C. Weast, Ed., "Handbook of Chemistry and Physics," 55th ed, Chemical Rubber Publishing Co., Cleveland, Ohio, 1974.

## Valence Level Photoelectron Spectra of Some Heavy Group 4-6 Diatomic Molecules

M. Wu and T. P. Fehlner\*

Contribution from the Department of Chemistry, University of Notre Dame, Notre Dame, Indiana 46556. Received March 26, 1976

**Abstract:** The He I photoelectron spectra of GeS, GeSe, SnS, SnTe, and PbTe in the gas phase have been obtained by the photoionization of the vapors above appropriate solids at temperatures ranging from 700 to 1000 K. Spectra are assigned using observed relative band areas, vibrational fine structure, and spin-orbit splitting along with electron impact ionization potentials and parallel mass spectrometric studies. It is demonstrated that there is significant mixing of the  $\Sigma_{1/2}$  and  $\Pi_{1/2}$  states in the heavier species. Distinct differences between the II states of light and heavy diatomics are observed. Similarities and differences between the valence regions of group 4-6 diatomics and diatomics of group 5-5 and group 3-7 are also reported.

Molecular photoelectron spectroscopy reveals the electronic structure of ions. It also provides an approximate, but valuable, representation of the filled molecular orbital structure of molecules.<sup>1</sup> As such it provides a really useful test of molecular orbital calculations.<sup>2</sup> The technique is most informative when applied to small molecules and small stable molecules have received much attention in the past.<sup>1</sup> Recently, the technique has been applied to less stable species, thereby

greatly increasing the number of small systems able to be studied.<sup>3</sup>

Our major objective in this work was to study the photoelectron spectra of the heavier congeners of CO in order to explore the electronic structure of diatomics in a region of the periodic table not readily accessible via calculation. Such species have been the subject of numerous studies utilizing mass spectrometry,<sup>4</sup> microwave spectroscopy,<sup>5</sup> and other

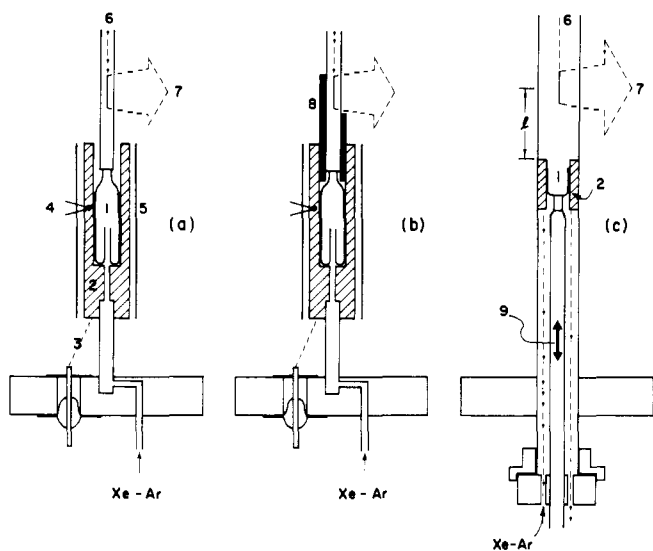


**Figure 1.** Schematic drawings of the furnaces used in the vaporization of group 4–6 solids: (1) quartz sample holder, (2) ceramic mount for non-inductively wound chromel resistance wire, (3) heater or thermocouple vacuum lead-through, (4) thermocouple, (5) tantalum foil radiation shield, (6) photon beam, (7) electron beam to energy analyzer, (8) copper sleeve, (9) direction of motion of the heater and sample holder in order to vary distance  $l$ .

techniques.<sup>6</sup> This work has demonstrated that the vapor over group 4–6 solids is a rich source of such diatomics and, thus, we have developed a photoelectron spectrometer capable of examining the vapor over solids at temperatures up to 1100 K.<sup>7</sup> Because both light and heavy group 4–6 diatomics can be examined, the results reported below provide an important link between previously reported studies on some covalent group 5–5 diatomics<sup>1,7,8</sup> and some heavy, group 3–7 diatomics.<sup>9,10</sup> Since beginning this report we have become aware of similar experimental work which resulted in the photoelectron spectra of GeS(g) and GeSe(g).<sup>11</sup>

The interesting question of the possible breakdown of the  $\sigma$ - $\pi$  orbital designation as spin-orbit interactions become more important is also approached in this study. Recently, Berkowitz has pointed out that the spectrum of Te<sub>2</sub> constitutes a departure from what he calls the principle of chemical similarity, i.e., molecules from the same column of the periodic chart tend to exhibit similar spectra.<sup>12</sup> The spectra reported herein provide another critical view of such expectations.

### Experimental Section

The photoelectron spectrometer used in previous studies<sup>13</sup> was adapted for the examination of high-temperature vapors in the following manner. Two separate integral furnaces, coaxial with the He I photon beam and situated in close proximity to the photoionization region, were constructed as illustrated in Figure 1. The device in Figure 1a,b had the advantage of allowing more controlled vaporization with some variation of the temperature of the photoionization region (by means of the copper sleeve shown in Figure 1b) at the expense of reduced sensitivity toward the less stable diatomics. The vaporization device in Figure 1c, however, allowed less controlled but more direct vaporization into the photoionization region. It also was constructed so that the distance between furnace and ionization region could be varied—a feature that was necessary for the observation of species of low stability. For example, the spectrum of GeCl<sub>2</sub> could be easily obtained in apparatus 1a and apparatus 1c with a furnace to ionization region distance of up to 3 cm.<sup>14</sup> However, PbTe could only be observed in apparatus 1c at a furnace to ionization distance of 0.5 cm.

Both furnaces were constructed from machinable ceramic and were heated by noninductively wound chromel wire driven by a dc power supply. Temperatures of the furnace walls were measured with Pt/Pt-10% Rh thermocouples, but little attempt was made to obtain

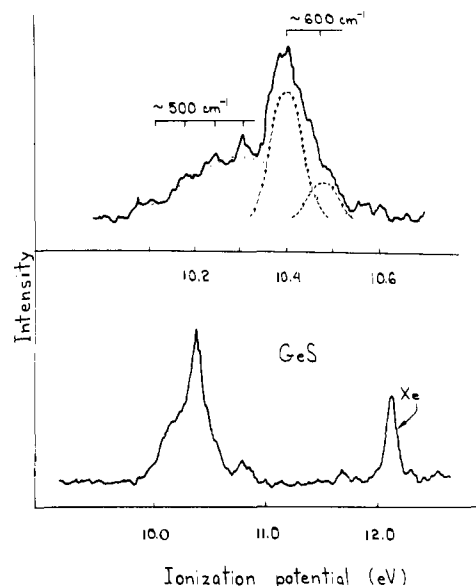


**Figure 2.** Photoelectron spectra of vapor above GeS(s). Using apparatus a in Figure 1. At the top of the figure the spectrum is shown under higher resolution.

accurate temperature measurements. The furnace in Figure 1a,b was shielded with 1 mil tantalum foil to reduce radiation losses. The furnaces could be operated at temperatures of up to 1200 K without significant interference with spectrometer operation.

The solids being vaporized were held in quartz vessels and the furnace temperature was raised slowly while monitoring the photoelectron spectrum. The spectra of the diatomics reported here were observed at temperatures ranging from 700 to 1000 K. In certain cases the spectrum of the species of interest could be enhanced by introducing a fairly large partial pressure of Xe in the furnace. Presumably this served to entrain the vapor and carry it into the photoionization region with a reduced number of wall collisions. This observation and the negative results on species such as GeTe lead us to believe that we are not looking at a true molecular beam of vaporized material.

The operating resolution of the spectrometer depended strongly on the deposition characteristics of the material being vaporized. The highest resolution achieved was 30-meV fwhm at 5-eV electron energy, while typical operating resolution was 40 meV at the same energy. Continuous calibration was carried out by flowing a Xe-Ar gas mixture through the furnace into the ionization region. This was necessary as large unpredictable shifts in the energy scale occurred during vaporization. These shifts did serve as a good indication of the temperature where vaporization was beginning. The spectrometer was scanned by varying the analyzer voltage and, when possible, data was accumulated in a multichannel analyzer.

As noted in the appropriate places below, many of the compounds studied here have been examined mass spectrometrically. In those cases where electron impact ionization potentials were unavailable or where mass spectrometric vaporization studies had not been reported, the appropriate compound was vaporized in a conventional manner utilizing a AEI MS 902 spectrometer for analysis. Electron impact ionization potentials were measured using either the linear extrapolation method or the extrapolated voltage difference method.<sup>15</sup>

The solids GeS, GeTe, and PbTe were obtained from K & K, GeS and GeSe from Pfalt & Bauer, SnS and SnTe from ROC/RIC and were used without further purification. In the case of one sample of GeS(s) an impurity problem was encountered. Here, heating at 600 K produced an intense HCl spectrum, which decreased after a period of hours. The three-band spectrum subsequently produced upon heating to 700 K was initially attributed by us to GeS(g), but we later showed it to be due to GeCl<sub>2</sub>(g).<sup>16</sup> The other sample of GeS(s) vaporized with no evidence of any significant impurities.

### Results and Discussion

**Vaporization of GeS(s).** Figure 2 illustrates the photoelectron spectrum of the vapor over solid GeS at a temperature of 700 K in the apparatus illustrated in Figure 1a. Other than a weak

**Table I.** The Vertical Ionization Potentials of GeS(g), GeSe(g), SnS(g), SnTe(g), and PbTe(g)

Band	GeS		GeSe		SnS		SnTe		PbTe	
	IP, eV	Ionic state	IP, eV	Ionic state	IP, eV	Ionic state	IP, eV	Ionic state	IP, eV	Ionic state
1	10.28	A <sup>2</sup> Π	9.95	A <sup>2</sup> Π <sub>3/2</sub> , A <sup>2</sup> Π <sub>1/2</sub>	10.20 <sup>a</sup>	χ <sup>2</sup> Σ, A <sup>2</sup> Π	8.65	A <sup>2</sup> Π <sub>3/2</sub>	8.04 <sup>b</sup>	A <sup>2</sup> Π <sub>3/2</sub>
2	10.39	χ <sup>2</sup> Σ	10.20	χ <sup>2</sup> Σ			8.95	A <sup>2</sup> Π <sub>1/2</sub>	8.34 <sup>b</sup>	A <sup>2</sup> Π <sub>1/2</sub>
3			13.4	B <sup>2</sup> Σ			9.39	χ <sup>2</sup> Π	9.01	χ <sup>2</sup> Σ
			14.9	C <sup>2</sup> Σ						

<sup>a</sup> This ionization potential corresponds to the center of the band, which most likely is a superposition of the χ<sup>2</sup>Σ and A<sup>2</sup>Π states. <sup>b</sup> See text.

**Table II.** Compilation of the First Vertical Ionization Potential Derived from Photoelectron Spectroscopic and Electron Impact Methods (eV)

	CO	SiO	GeO	SnO	PbO
PES	14.01 <sup>a</sup>				
EI		11.58 ± 0.1 <sup>b</sup>	11.10 ± 0.1 <sup>b</sup> 10.1 ± 0.8 <sup>c</sup>	10.5 ± 0.5 <sup>d</sup>	9.0 ± 0.5 <sup>e</sup>
	CS	SiS	GeS	SnS	PbS
PES	11.31 <sup>f</sup>		10.25 <sup>h</sup>	10.20 <sup>i</sup>	
EI	11.8 ± 0.2 <sup>g</sup>		10.9 ± 0.5 <sup>h</sup>	9.7 ± 0.5 <sup>k</sup>	8.6 ± 0.5 <sup>k</sup>
		GeSe	SnSe	PbSe	
PES		9.95 <sup>h</sup>			
EI		10.2 ± 0.5 <sup>h</sup>	9.7 ± 0.5 <sup>j</sup>		
		GeTe	SnTe	PbTe	
PES			8.65 <sup>h</sup>	8.19 <sup>h</sup>	
EI			9.1 ± 0.5 <sup>j</sup>	8.2 ± 0.5 <sup>l</sup>	

<sup>a</sup> Reference 1. <sup>b</sup> Reference 4. <sup>c</sup> J. Drowart, F. Degreve, G. Verhaegen, and R. Colin, *Trans. Faraday Soc.*, **61**, 1072 (1965). <sup>d</sup> R. Colin, J. Drowart, and G. Verhaegen, *Trans. Faraday Soc.*, **61**, 1364 (1965). <sup>e</sup> J. Drowart, R. Colin, and G. Exsteen, *Trans. Faraday Soc.*, **61**, 1367 (1965). <sup>f</sup> Reference 27. <sup>g</sup> L. P. Blanchard and P. LeGoff, *Can. J. Chem.*, **35**, 89 (1957). <sup>h</sup> This work. <sup>i</sup> This energy corresponds to the center of the observed band, which most likely is a superposition of σ and π ionizations. <sup>j</sup> Reference 37. <sup>k</sup> R. Colin and J. Drowart, *J. Chem. Phys.*, **37**, 1120 (1962). <sup>l</sup> Reference 39.

band identified as H<sub>2</sub>O, the spectrum under low resolution exhibits a single unknown band distorted on the low ionization side (Figure 2, bottom). This spectrum is similar to that reported elsewhere.<sup>11</sup> Under highest resolution (Figure 2, top), the band is resolved into a sharp component at vertical ionization potential of 10.39 eV and a broad component at vertical ionization potential of 10.28 eV with areas in the ratio of 1:1.3 (see Table I). These are assigned to the ionization of the GeS molecule for three reasons. First, in a separate experiment, the vaporization of GeS(s) was examined with mass spectrometric analysis of the vapor. The major constituent of the vapor is GeS(g). Second, in the mass spectrometric experiments, the electron impact appearance potential of GeS<sup>+</sup> ion is measured to be 10.9 ± 0.5 eV, which is consistent with the ionization potential of the complex band in the photoelectron spectrum of GeS(g). Finally, as indicated by the ionization potentials gathered in Table II, the first ionization potential of GeS(g) fits into the smooth trend of decreasing ionization potential with increasing atomic number.

In the valence region, GeS should have two σ levels and one π level. As ionization probabilities for closed shell species are approximately proportional to the occupation number of the orbital,<sup>17</sup> the bands corresponding to these types of ionization should have approximate relative intensities of 1:2. On this basis we would tend to assign the band at 10.28 eV to ionization of the lowest π-type orbital and the band at 10.39 eV to ion-

ization of the σ-type orbital. The vibrational structure in the two bands is consistent with this assignment (see below). The other expected σ ionization, however, could not be located. However, as pointed out below in the discussion of GeSe(g), this band will have lower net relative intensity and, in addition, will be split into two bands. Thus, the third band expected here is probably lost in the noise.

Considerable effort was devoted to obtaining sufficient instrumental resolution in order to observe vibrational fine structure. In the spectrum at the top of Figure 2, the resolution (fwhm) at 10 eV under operating conditions was about 70 meV, which is comparable to the vibrational frequency of GeS (575 cm<sup>-1</sup>).<sup>18</sup> Under these conditions vibrational structure should be evident on the σ band. However, vibrational structure on the π band will tend to be obscured as each vibrational component will be split by a spin-orbit interaction of 300–400 cm<sup>-1</sup>.<sup>19</sup> The band at lowest ionization potential at the top of Figure 2 does appear to exhibit a vibrational progression with a spacing of about 500 cm<sup>-1</sup>. This suggests the assignment of this band to the χ<sup>2</sup>Σ state of GeS<sup>+</sup>; however, this reasoning is unacceptable as deconvolution of the sharp band at 10.39 eV into symmetrical components with fwhm equal to the instrumental resolution reveals two vibrational components with a splitting of about 600 cm<sup>-1</sup>. The dilemma would be resolved if there is little mixing of the S 2p orbitals with Ge 2p orbitals in the π state such that the spin-orbital splitting is 440 cm<sup>-1</sup>

(the value of  $\text{CS}_2$  with localization on sulfur).<sup>1</sup> The broad band could then be assigned to the  $A^2\Pi$  state, each fine structure line consisting of unresolved  $\Pi_{3/2\nu_n}$  and  $\Pi_{1/2\nu_{n+1}}$  components.<sup>20</sup> The sharp band would then be necessarily assigned to the  $\chi^2\Sigma$  state of  $\text{GeS}^+$ .

If this assignment is correct it would suggest a small increase in bond length in going from the molecule to the  $A^2\Pi$  ionic state and a small decrease in bond length in going to the  $\chi^2\Sigma$  ionic state. This is qualitatively similar to the situation with CO and CS. However, the envelope of the band assigned to the  $A^2\Pi$  state of  $\text{GeS}^+$  is considerably narrower than similar bands in CO and CS. This would suggest less  $\pi$ -type interaction between the group 4 and group 6 atoms in GeS compared to CS and CO, which is consistent with the assumption made in assigning the bands. It is also consistent with the smaller change in vibrational separation in going from GeS to the  $A^2\Pi$  state of  $\text{GeS}^+$  compared to similar transitions in CO and CS.

The characteristics of analogous bands in some group 3–7 diatomics have been explained using a model that focuses on the ionic character of these molecules.<sup>9,10</sup> This ionic bond model has been generally accepted;<sup>21</sup> however, it should be pointed out that this model does fail in the case of BF. The antibonding character of the  $\chi^2\Sigma$  ionic state of BF has been established by both experimental work<sup>22</sup> and theoretical calculations.<sup>23</sup> The dipole moment of BF is  $-1.0$  D with a net negative charge on boron.<sup>5</sup> Thus, the ionic bond model would predict that the removal of an electron from the outermost  $5\sigma$  orbital, which is localized on the boron atom, would produce an increase in the bond length rather than the decrease in bond length expected on the basis of the known antibonding character of this orbital.

Thus, we would like to suggest an alternative qualitative explanation of the observed antibonding character of the  $\chi^2\Sigma$  state of GeS. It has been suggested, on the basis of calculations utilizing the Hellmann–Feynmann theorem, that the distribution of molecular charge can be assigned to *binding* and *antibinding* regions as illustrated in Figure 3.<sup>24</sup> These regions are defined such that electronic charge in the binding region exerts a net force that tends to shorten the internuclear distance. Charge in the antibinding region has the opposite effect. Ionization that causes a relative reduction in the electronic charge in the binding region will result in an increased internuclear distance in the ion and the ionization process would then be classified in the terms of the photoelectron spectroscopist as the removal of a bonding electron. Relative removal of antibinding charge would result in classification of the band as resulting from the removal of an antibonding electron. As polarity is introduced into the diatomic, the antibinding region behind the nucleus of higher nuclear charge expands, while that behind the nucleus of smaller charge shrinks (Figure 3). This is readily understandable, as the direction of net force on the nuclei caused by a unit of charge at a fixed position depends on the effective nuclear charges at this position. Finally, as charge densities of different orbitals lie in different regions of space, this binding–antibinding division can be used to rationalize the character of the associated bands in the photoelectron spectra.

For example, the  $5\sigma$  ionizations in  $\text{N}_2$ , CO, and BF are empirically characterized as bonding, nonbonding, and antibonding, respectively.<sup>1,22,23</sup> As one goes from  $\text{N}_2$  to CO, part of the  $5\sigma$  overlap charge density in the binding region is transferred to the antibinding region behind the carbon nucleus. In going from CO to BF this transfer of charge density behind the less electronegative element is further increased; however, because of the reduced size of the antibinding region behind boron the small transfer to the antibinding region behind fluorine should not be neglected. This is readily evident from a consideration of qualitative orbital maps.<sup>25,26</sup> Thus, the increasing localization of the  $5\sigma$  orbital on the electropositive

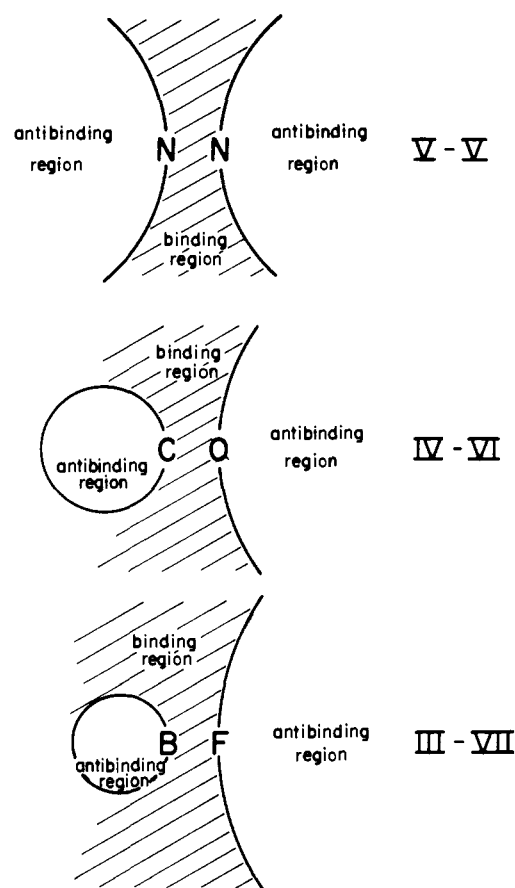


Figure 3. Qualitative division of space around diatomic molecules into binding and antibinding regions after Berlin (ref 24).

element as the polarity of the molecule increases predicts an increasing antibonding character for the corresponding ionization in the series  $\text{N}_2 > \text{CO} > \text{BF}$  as observed. This qualitative conclusion is confirmed by quantitative orbital force analysis in these three diatomics, in which separate examinations of the binding force exerted by the individual molecular orbitals are carried out.<sup>25</sup>

This analysis can also be used to rationalize the character of the  $7\sigma$  ionization in CS. Although the dipole moment of this species is negative ( $-1.6$  D),<sup>5</sup> the vibrational lines in the band associated with the  $7\sigma$  ionization exhibit a spacing of  $1384$   $\text{cm}^{-1}$  relative to  $1272$   $\text{cm}^{-1}$  in the neutral molecule.<sup>27</sup> Again this is inconsistent with the ionic bond model, but it is readily explained in terms of dividing charge into binding–antibinding parts. The  $7\sigma$  orbital has a strong  $2p\sigma$  character,<sup>28</sup> thus, ionization removes charge density mainly from the antibinding region behind the carbon nucleus, thereby shortening the bond length and increasing the vibrational frequency.

Similarly, then, we suggest that the antibonding character exhibited by GeS in the ionization of the highest occupied  $\sigma$  orbital results from charge localization in the antibinding region behind the Ge nucleus. That is, even though the antibonding character could be explained by the ionic bond model (the dipole moment of GeS is  $2.0$  D),<sup>5</sup> we suggest that the character of the ionization is better related to the charge distribution in the binding and antibinding regions rather than the overall dipole moment.

**Vaporization of GeSe(s).** The spectrum illustrated in Figure 4 was obtained with little difficulty by the vaporization of GeSe(s) at  $800$  K in apparatus 1a and is similar to that produced by others.<sup>11</sup> As indicated in Table I, the vertical ionization potentials of the components of the strongest band are  $9.95$  and  $10.20$  eV. These are assigned to the ionization of GeSe(g) for the following reasons. First, the vaporization of

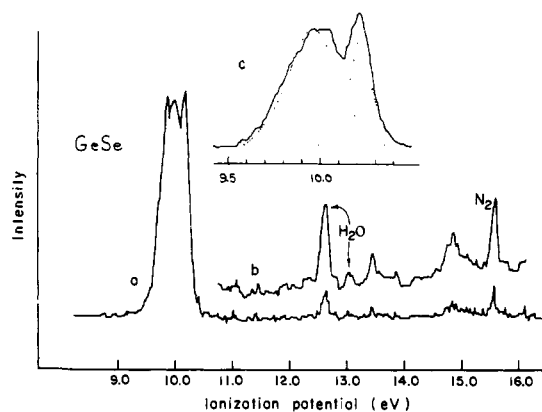
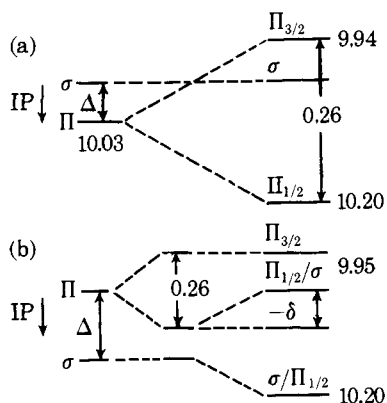


**Figure 4.** Photoelectron spectra of vapor above GeSe(s) using apparatus a in Figure 1: (a) wide scan, (b) spectrum,  $a \times 10$ , (c) lowest ionization under higher resolution.

GeSe(s) is known to be congruent.<sup>29</sup> Second, previous microwave experiments<sup>5</sup> have established the relative stability of GeSe(g) and the major decomposition product, Se<sub>2</sub>, has a rather different spectrum.<sup>30</sup> Third, in separate experiments, the vapor over GeSe(s) was examined mass spectrometrically, thereby confirming the vapor composition of GeSe. The appearance potential of the GeSe<sup>+</sup> ion was measured to be  $10.2 \pm 0.5$  eV using the extrapolated voltage difference method. This value compares favorably with the energy of the first band in the photoelectron spectrum. Finally, the first ionization potential correlates well with the ionization potentials of other group 4–6 diatomics (Table II).

As there is only one strong band in Figure 4, the highest occupied  $\sigma$  and  $\pi$  levels must lie close together. The  $\pi$  orbital is expected to have a splitting of  $\leq 0.26$  eV, since this is the spin-orbit splitting of the  $\chi^2\Pi$  ionic state of CSe<sub>2</sub> in which there is 100% Se localization.<sup>31</sup> There are two reasonable assignments of these bands, which are shown schematically in Scheme I. The difference in these two assignments is that one

#### Scheme I



(b) allows an interaction ( $\delta$ ) between the  $\Sigma_{1/2}$  state and the  $\Pi_{1/2}$  state, which have like symmetries in terms of the double group.<sup>32</sup> It has been pointed out that the interaction parameter for such mixing should be  $\xi/\sqrt{2}$ , where  $\xi$  is the spin-orbit splitting and where there is a predominant p-type interaction.<sup>33</sup> Thus, if  $\Delta$  is such that the  $\Sigma_{1/2}$  and  $\Pi_{1/2}$  states lie close to one another, an interaction is possible. Note that both assignments allow a  $\Pi_{3/2}, \sigma, \Pi_{1/2}$  ordering, while (a) allows  $\sigma, \Pi_{3/2}, \Pi_{1/2}$  and (b) allows a  $\Pi_{3/2}, \Pi_{1/2}, \sigma$  ordering, depending on the magnitude of  $\Delta$ . An unambiguous assignment is not possible; however, the spectrum places limits on  $\Delta$ . The level at 10.20 eV is clearly fixed, the level at lowest ionization potential cannot be less than 9.85 eV, and the middle level cannot lie

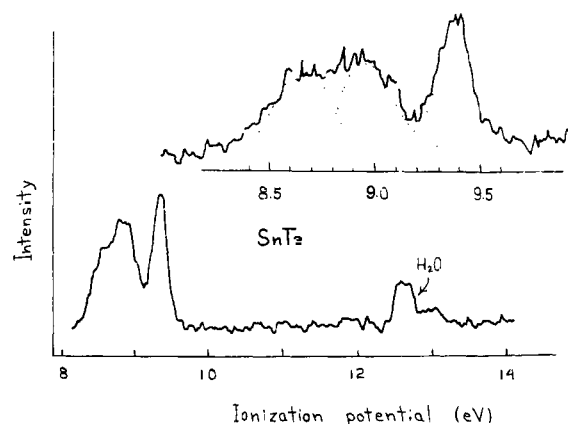


**Figure 5.** Photoelectron spectra of vapor above SnTe(s) using apparatus b in Figure 1. At the top of the figure the spectrum is shown under higher resolution.

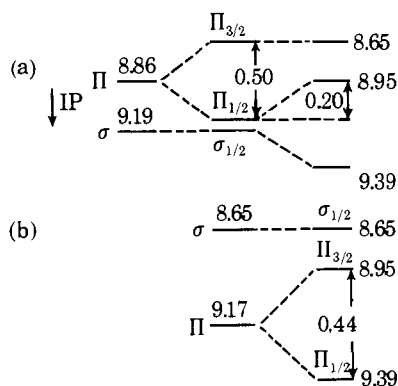
higher than 10.05 eV. This leads to a maximum  $\Delta$  of 0.22 eV for assignment 2 with ordering  $\sigma, \Pi_{3/2}, \Pi_{1/2}$  to a minimum  $\Delta$  of  $-0.16$  eV for assignment b with ordering  $\Pi_{3/2}, \Pi_{1/2}, \sigma$  and  $\delta = 0.06$  eV. Despite the risk of putting too much emphasis on state labels, we prefer the assignment with  $\Delta = -0.16$  eV,  $\delta = 0.06$  eV, as it is most consistent with our other results.

As pointed out above another  $\sigma$  level is expected in the valence region. There are two weak bands at about 13.4 and 14.9 eV, a small part of the latter band intensity being due to the second band of the small water impurity. One of these bands is attributed to the  $B^2\Sigma$  ionic state of GeSe(g), while the other is attributed to a “shake-up” band,<sup>34</sup> i.e., a state pictured as resulting from ionization plus excitation. This is similar to the situation that obtains in the case of CS.<sup>27,28</sup> The low intensities are due to two factors. First, large, outer orbitals have greater cross sections than inner orbitals<sup>35</sup> and, second, the total intensity expected in the other valence  $\sigma$  level is now split between the observed  $\Sigma$  state and the “shake-up” band.<sup>36</sup>

**Vaporization of SnTe(s).** The photoelectron spectrum of the vapor above SnTe(s) in apparatus 1b at 1000 K is presented in Figure 5. Two bands are observed. The band at lower ionization energy appears to have two components centered at 8.61 and 8.89 eV, while the band at 9.39 eV appears singular. Observations similar to those presented above for GeS(g) and GeSe(g) allow these bands to be assigned to SnTe(g). First, attributing these bands to SnTe is consistent with the known composition and stability of the vapor over SnTe(s).<sup>5,6,37</sup> Second, electron impact ionization potential measurements yield a value of  $9.1 \pm 0.5$  eV for the lowest vertical ionization potential of SnTe(g).<sup>37</sup> This agrees within experimental error with the mean energy of the first band. Third, the temperature dependence of the bands is consistent with the vaporization of a single species. Finally, the first ionization potential correlates well with that of other group 4–6 diatomics (Table II).

The two bands in Figure 5 attributed to SnTe(g) result from ionization from the highest occupied  $\sigma$  and  $\pi$  levels. The other  $\sigma$  band expected is either lost in the substantially higher background, due to loss of intensity to “shake-up” bands (see above), or obscured by the water impurity. There are two reasonable assignments shown schematically in Scheme II. These two assignments differ in the relative energies of the original  $\sigma$  and  $\pi$  levels and in the requirement in (a) for a significant  $\Sigma_{1/2}-\Pi_{1/2}$  interaction. In both cases the magnitude of the spin-orbit splitting is taken to be 0.5 eV, a value observed in Te<sub>2</sub>.<sup>12</sup> We prefer the first assignment, as group 5–5, group 3–7, and CO, CS, GeS, and GeSe exhibit a uniformly decreasing energy of the  $\pi$  level with respect to the first  $\sigma$  level. In fact, in the series N<sub>2</sub>, PN, P<sub>2</sub>, there is an unambiguous crossover of the  $\sigma$  and  $\pi$  levels.<sup>1,7,8</sup> Thus, it seems unlikely that

Scheme II

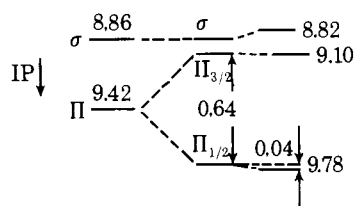


there should be a sudden change in behavior in the case of SnTe.

As noted in the discussion of GeSe, the  $\Sigma_{1/2}-\Pi_{1/2}$  interaction parameter is expected to be  $\xi/\sqrt{2}$  for p-type interaction. The parameter called for by assignment a is 0.22 eV, which is about 40% smaller than the expected value.

It is interesting to compare the spectrum of SnTe(g) to that of the isoelectronic group 3-7 analogue, InI(g) which has been reported by others.<sup>10</sup> Everything seems to be reversed in InI. The first band is the most intense band and appears to have two components, the one at lower ionization potential being assigned to ionization from the  $\Sigma_{1/2}$  state and the higher to the  $\Pi_{3/2}$  state. The second band has one component, assigned to  $\Pi_{1/2}$ , with an intensity slightly higher than that assigned to the  $\Pi_{3/2}$  level. The schematic assignment given was that shown in Scheme III. It will be noted in this case that the  $\Sigma_{1/2}-\Pi_{1/2}$

Scheme III



interaction increases the observed  $\Pi_{3/2}-\Pi_{1/2}$  separation, whereas in the case of SnTe it decreases this separation. This is qualitatively evident from a comparison of the spectra. The calculated  $\Sigma_{1/2}-\Pi_{1/2}$  interaction parameter for InI is 0.2 eV compared with 0.45 eV expected for a pure p-type interaction. Note that the value of the measured parameter is uncertain, as the  $\Pi_{3/2}$  state appears as a weak shoulder on the high energy side of the first band.

**Vaporization of PbTe(s).** The vaporization of PbTe in apparatus 1a,b yielded only the spectrum of Te<sub>2</sub>. The spectrum of this species has already been reported by others<sup>12</sup> and was also obtained in this work during the vaporization of GeTe(s).<sup>38</sup> Thermogravimetric investigations, however, have indicated that the overall complexity of vaporization increases in the series PbTe, SnTe, GeTe rather than the reverse.<sup>6</sup> We suspected that the observed decomposition might be due to the lower dissociation energy of PbTe(g) relative to that of SnTe(g). Thus, PbTe(s) was vaporized in the device that minimizes like gas collisions (Figure 1c). At about 1000 K, with a distance of 0.5 cm between crucible and ionization zone and at relatively high Xe pressures, the spectrum in Figure 6 was obtained. This spectrum is attributed to PbTe(g) because of the rather rigorous conditions necessary to see it, because the electron impact ionization potential ( $8.2 \pm 0.5$  eV<sup>39</sup>) agrees within experimental error with the vertical ionization potential of the first photoelectron band, and because of the correlations of Table II.

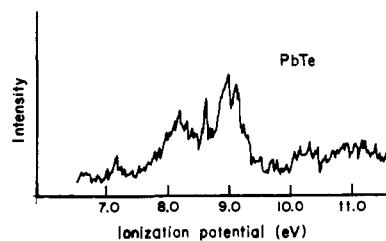
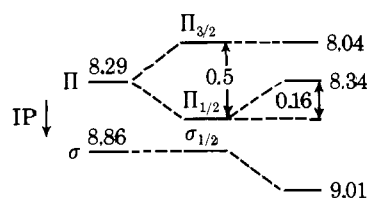


Figure 6. Photoelectron spectrum of the vapor above PbTe(s) using apparatus c in Figure 1.

The quality of this spectrum is lower than those discussed above, but clearly there are two bands present, which may be assigned to the highest occupied  $\sigma$  and  $\pi$  levels. Again the other  $\sigma$  band is not observed, but for the same reasons given in the case of SnTe(g), this is not unexpected. Our assignment of this spectrum proceeds logically from the assignments of GeS, GeSe, and the preferred assignment of SnTe(g). In schematic form it is shown in Scheme IV. The  $\Sigma_{1/2}-\Pi_{1/2}$  interaction

Scheme IV



parameter is 0.29 eV, approximately equal to that for SnTe. Such an assignment assumes that the band at lowest ionization potential is actually two bands. Verification would require a better spectrum. This, unfortunately, is outside of our present capabilities.

Here, too, we may compare the spectrum of PbTe(g) with its group 3-7 analogue TlI(g), which has been reported previously.<sup>9</sup> Like the SnTe-InI pair, everything appears reversed in the PbTe-TlI comparison. Again it is qualitatively evident from a comparison of the spectra that in the case of PbTe the  $\Sigma_{1/2}-\Pi_{1/2}$  interaction decreases the  $\Pi_{3/2}-\Pi_{1/2}$  separation, whereas in the case of TlI it increases the separation. For TlI, the calculated  $\Sigma_{1/2}-\Pi_{1/2}$  interaction parameter is 0.30 eV compared with 0.45 eV expected for pure p interaction.

**Vaporization of SnS(s).** Because of the known lower stability of SnS(g),<sup>5</sup> the vaporization of SnS(s) was examined in apparatus 1c only. At the minimum crucible to ionization zone distance, at high Xe pressures, and at ca. 950 K, the spectra similar to those illustrated in Figure 7 were obtained. Bands are observed at about 9.55 and 10.20 eV and the relative intensities of these bands depend strongly on vaporization conditions, which is indicative of the production of two species. The band at 9.55 eV is associated with the more stable of the two species and further work<sup>38</sup> in these laboratories along with previously published spectra<sup>12,40</sup> allows the assignment of this band to the ionization of S<sub>2</sub>(g). The other band is attributed to the ionization of SnS(g) because of the stringent conditions necessary to observe it (particularly the dependence on Xe "carrier" gas), because the electron impact ionization potential ( $9.7 \pm 0.5$  eV) agrees with the ionization energy of the center of the observed band, and because of the correlations in Table II.

This is the poorest quality spectrum of all the diatomics discussed and would not have been included except to make one important qualitative point. The breadth of the observed band attributed to SnS(g) and the absence of any other bands in the 10-12-eV region strongly suggest that the  $\sigma-\pi$  separation is small. As will be seen below, this conclusion is consistent

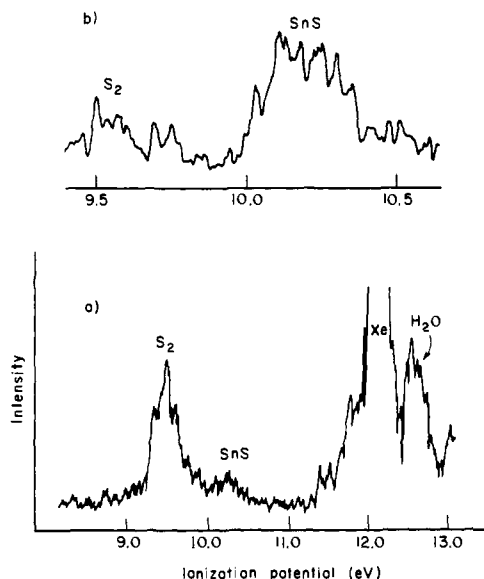


Figure 7. Photoelectron spectra of the vapor above SnS(s) using apparatus c in Figure 1, spectrum a being at the higher temperature.

with the observations reported on the other group 4-6 diatomics.

**Vaporization of Other Solids.** The vaporization of SnSe(s), GeTe(s), GeO(s), and SiS(s) has also been examined. Either the group 6-6 disproportionation product was observed (i.e., Se<sub>2</sub>, Te<sub>2</sub>, S<sub>2</sub>) or the bands could not be definitely attributed to the group 4-6 species desired. These results qualitatively verify the stability order described by others.<sup>5</sup>

### Conclusions

In Figure 8 the trends in the group 4-6  $\sigma$ - $\pi$  energy separations, computed for each molecule as indicated above, are compared to those for group 5-5 and group 3-7 diatomics. Three points deserve comment. First, in each of the three cases the  $\sigma$ - $\pi$  separation decreases with increasing atomic number. This is understandable in a qualitative sense in terms of the Mulliken united atom correlation diagram for diatomics.<sup>41</sup> The highest filled  $\sigma$  and  $\pi$  orbitals (the  $x\sigma$  and  $w\pi$  for CO orbitals in Mulliken's notation) correlate with  $l = 1$  levels in the united atom, which differ in quantum number  $n$  by one. As the atomic number increases the difference in energy between shells decreases, requiring a similar decrease in  $\sigma$ - $\pi$  separation. This model cannot explain the observed crossover of the  $\sigma$ - $\pi$  levels observed for groups 5-5 and 4-6. Such a crossover suggests significant s character in the  $\sigma$  level—a suggestion that also resulted from the analysis of the  $\Sigma_{1/2}$ - $\Pi_{1/2}$  mixing in the heavier group 4-6 molecules.

The second point to notice in regard to Figure 8 is that the  $\sigma$ - $\pi$  separation at a given  $Z$  depends strongly on the polarity of the diatomic molecule and increases in the order group 5-5 > group 4-6 > group 3-7. This may be understood in terms of a greater localization of the highest filled  $\sigma$  orbital on the more electropositive atom as the  $\pi$  orbital becomes localized on the more electronegative atom as one proceeds from 5-5 to 4-6 to 3-7. Again this is expected in terms of the united atom model.

The third point involves a comparison of the light vs. the heavy group 4-6 species. The trend in the  $\sigma$ - $\pi$  separation for CO and CS follows that for N<sub>2</sub>, PN, and P<sub>2</sub>, whereas the trend for the heavy 4-6 molecules corresponds more closely to that for the heavy 3-7 molecules. It was pointed out above that there is a difference between the  $\pi$  bands in CO and CS and the analogous bands in the heavier group 4-6 molecules; the former being characteristic of the removal of a bonding elec-

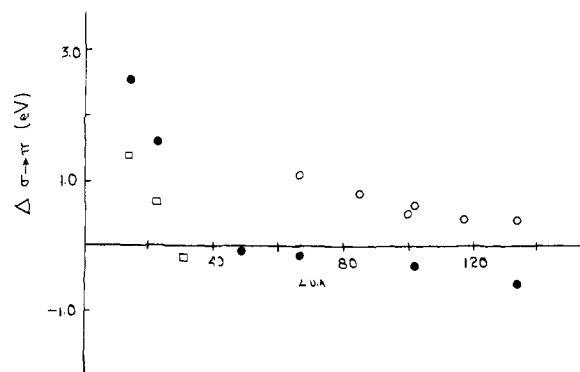


Figure 8. A plot of the  $\sigma$ - $\pi$  separation of group 5-5 ( $\square$ ), 4-6 ( $\bullet$ ), and 3-7 ( $\circ$ ) diatomic molecules as a function of  $Z$ , where  $Z$  is the atomic number of the united atom formed by the molecule. Data for the group 5-5 molecules are from ref 1, 7, and 8, that for CO and CS from ref 1 and 27, and that for the group 3-7 molecules from ref 9 and 10.

tron, while the latter were characteristic of the removal of a more nonbonding electron. Thus, we suggest that the precipitous decrease in the  $\sigma$ - $\pi$  separation for the light molecules is due to a rapid decrease in the  $\pi$  interaction between the two atoms ( $\pi$  bonding), while the more gentle decrease for the heavier molecules is attributed to relative shielding effects.<sup>42</sup> If so, simple extrapolation would suggest that the 4-6  $\pi$  interaction is small above  $Z = 35$ .

Finally, the fact that the  $\sigma$ - $\pi$  separations correlate well as  $Z$  increases to large values indicates that the  $\sigma$ - $\pi$  concept is still a useful one for molecules containing atoms of large  $Z$ , despite the fact that the electronic states themselves are only poorly represented by such a description. Thus, although the principle of chemical similarity is not immediately obvious from an inspection of the spectra, it still constitutes a foundation for understanding these spectra.<sup>43</sup>

**Acknowledgment** is made to the donors of the Petroleum Research Fund, administered by the American Chemical Society, for the support of this research. We also wish to thank Dr. J. Berkowitz and Professor J. Drowart for communicating results prior to publication.

### References and Notes

- (1) D. W. Turner, C. Baker, A. D. Baker, and C. R. Brundle, "Molecular Photoelectron Spectroscopy", Wiley-Interscience, New York, N.Y., 1970.
- (2) See, for example: H. Bock and B. G. Ramsey, *Angew. Chem. Int. Ed. Engl.*, **12**, 734 (1973).
- (3) (a) J. Berkowitz in "Electron Spectroscopy: Theory, Technique, and Application", Academic Press, London, in press; (b) G. K. Schweitzer, *Appl. Spectrosc. Rev.*, **10**, 257 (1975).
- (4) See, for example: D. L. Hildenbrand, *Int. J. Mass Spectrom. Ion Phys.*, **7**, 255 (1971).
- (5) J. Hoelt, F. J. Lovas, E. Tiemann, and T. Törring, *J. Chem. Phys.*, **53**, 2736 (1970).
- (6) D. A. Northrop, *J. Phys. Chem.*, **75**, 118 (1971).
- (7) M. Wu and T. P. Fehlner, *Chem. Phys. Lett.*, **36**, 114 (1975).
- (8) A. W. Potts, K. G. Glenn, and W. C. Price, *Discuss. Faraday Soc.*, **54**, 65 (1972).
- (9) J. Berkowitz, *J. Chem. Phys.*, **56**, 2766 (1972).
- (10) J. Berkowitz and J. L. Dehmer, *J. Chem. Phys.*, **57**, 3194 (1972).
- (11) R. Peeters, Ph.D. Thesis, The Free University of Brussels, 1975, and J. Drowart, The Free University of Brussels, personal communication, 1976.
- (12) J. Berkowitz, *J. Chem. Phys.*, **62**, 4074 (1975).
- (13) T. P. Fehlner, *Inorg. Chem.*, **14**, 934 (1975).
- (14) M. Wu and T. P. Fehlner, unpublished data.
- (15) R. W. Kiser, "Introduction to Mass Spectrometer and Its Application", Prentice-Hall, Englewood Cliffs, N.J., 1965.
- (16) We thank Professor Drowart for sending us a copy of a thesis containing a spectrum of GeS(g), thereby drawing our attention to this error.
- (17) P. A. Cox and A. F. Orchard, *Chem. Phys. Lett.*, **7**, 273 (1970).
- (18) C. V. Shapiro, R. C. Gibbs, and A. W. Laubengayer, *Phys. Rev.*, **40**, 354 (1932).
- (19) The observed spin-orbit splitting in HBS, for example, is about 300 cm<sup>-1</sup>. T. P. Fehlner and D. W. Turner, *J. Am. Chem. Soc.*, **95**, 7175 (1973).
- (20) The first vibrational component could be a hot band, i.e., ionization of GeS in the first vibrational state. From the furnace temperature one predicts

- a maximum relative population of this state of 21% of the ground state. If this is the case then the band is actually "sharper" than it appears.
- (21) J. H. D. Eland, "Photoelectron Spectroscopy", Wiley, New York, N.Y., 1974.
- (22) R. B. Caton and A. E. Douglas, *Can. J. Phys.*, **48**, 432 (1970).
- (23) R. K. Nesbet, *J. Chem. Phys.*, **43**, 4403 (1965).
- (24) T. Berlin, *J. Chem. Phys.*, **19**, 208 (1951).
- (25) R. F. W. Bader and A. D. Bandrauk, *J. Chem. Phys.*, **49**, 1653 (1968).
- (26) W. M. Huo, *J. Chem. Phys.*, **43**, 624 (1965).
- (27) N. Jonathan, A. Morris, M. Okuda, D. J. Smith, and K. J. Ross, *Chem. Phys. Lett.*, **13**, 334 (1972); C. H. King, H. W. Kroto, and R. J. Suffolk, *Chem. Phys. Lett.*, **13**, 457 (1972); N. Jonathan, A. Morris, M. Okuda, K. J. Ross, and D. J. Smith, *Discuss. Faraday Soc.*, **54**, 48 (1972); D. C. Frost, S. T. Lee, and C. A. McDonald, *Chem. Phys. Lett.*, **17**, 153 (1972); M. Okuda and N. Jonathan, *J. Electromagn. Spectrosc. Relat. Phenom.*, **3**, 19 (1974).
- (28) W. G. Richards, *Trans. Faraday Soc.*, **63**, 257 (1967).
- (29) L. Chun-Hau, R. S. Pashinkin, and A. V. Novoselova, *Russ. J. Inorg. Chem.*, **7**, 496 (1962).
- (30) The spectrum of  $(\text{Se})_n$ , including  $\text{Se}_2$  was produced by the vaporization of  $\text{GeSe}_2$ .  $\text{Se}_2$  was also produced in the vaporization of  $\text{SnSe}(s)$ : M. Wu, unpublished data. The spectrum of  $\text{Se}_2$  has also been communicated to us by J. Berkowitz.
- (31) D. C. Frost, S. T. Lee, and C. A. McDowell, *J. Chem. Phys.*, **59**, 5484 (1973).
- (32) G. Herzberg, "Molecular Spectra and Molecular Structure. III. Electronic Spectra and Electronic Structure of Polyatomic Molecules", Van Nostrand, Princeton, N.J., 1966.
- (33) J. Berkowitz, J. L. Dehmer, and T. E. H. Walker, *J. Chem. Phys.*, **59**, 3645 (1973).
- (34) S. Cradock and W. Duncan, *Mol. Phys.*, **27**, 837 (1974).
- (35) A. W. Potts and W. C. Price, *Proc. R. Soc. London, Ser. A*, **326**, 165 (1972).
- (36) S. Cradock and W. Duncan, *J. Chem. Soc., Faraday Trans. 2*, **71**, 1262 (1975).
- (37) R. Colin and J. Drowart, *Trans. Faraday Soc.*, **60**, 673 (1964).
- (38) M. Wu and T. P. Fehlner, unpublished work.
- (39) R. F. Porter, *J. Chem. Phys.*, **34**, 583 (1961).
- (40) J. M. Dyke, L. Golob, N. Jonathan, and A. Morris, *J. Chem. Soc., Faraday Trans. 2*, 1026 (1975).
- (41) G. Herzberg, "Molecular Spectra and Molecular Structure. I. Spectra of Diatomic Molecules", Van Nostrand, Princeton, N.J., 1950.
- (42) A recent calculation [D. P. Chong, F. G. Herring, and D. P. McWilliams, *J. Electron Spectrosc. Relat. Phenom.*, **7**, 429 (1975)] indicates a  $\sigma$ - $\pi$  separation in BF of 8.7 eV. The fact that it is quite large is consistent with the trends illustrated in Figure 8.
- (43) NOTE ADDED IN PROOF. The valence level photoelectron spectrum of  $\text{Bi}_2$  has recently been reported (S. Süzer, S. T. Lee, and D. A. Shirley, *J. Chem. Phys.*, **65**, 412 (1976)). The  $\sigma$ - $\pi$  separation is  $-1.07$  eV for a  $Z_{\text{UA}}$  of 166. Thus, the behavior exhibited in Figure 8 for group 4-6 molecules is paralleled by group 5-5 molecules.

## Photoelectron Spectroscopy of Bis( $\pi$ -allyl)nickel and Its Methyl Substituted Derivatives: Support for the Near Validity of Koopmans' Theorem

Christopher D. Batich<sup>1</sup>

*Physikalisch-chemisches Institut der Universität Basel, CH-4056 Basel, Switzerland, and the Max-Planck Institut für Kohlenforschung, 433 Mülheim a.d. Ruhr, West Germany. Received May 3, 1976*

**Abstract:** The He (I) photoelectron spectra of bis( $\pi$ -methallyl)nickel, bis( $\pi$ -crotyl)nickel, and bis( $\pi$ -1,3-dimethylallyl)nickel are presented and related to bis( $\pi$ -allyl)nickel (**1**). It is shown that a previous assignment for **1** should be modified by placing the  $\pi(a_u)$  ionization energy within 0.4 eV of the first ionization energy. This new assignment substantially reduces the continuing disagreement between experiment and theoretical Koopmans type calculations. Methyl substituent effects are shown to be useful in assigning photoelectron spectra of organometallic systems. A detailed discussion of the assignment criteria is presented which includes a He (II) spectrum of bis( $\pi$ -methallyl)nickel.

Transition metal complexes involving the allyl radical as a three-electron ligand represent the simplest "sandwich" compounds known. Because of this, and their extensive and interesting chemistry,<sup>2-4</sup> they are an obvious choice for the application of theoretical methods to organometallic systems. Although the mode of bonding has been discussed in general books on the subject,<sup>5,6</sup> only a description couched in broad terms could be used because of uncertainties about relative energies of the occupied molecular orbitals. Recently a number of theoretical methods have been used to calculate the electronic structure of bis( $\pi$ -allyl)nickel (**1**); among them: SCCC MO (self-consistent charge and configuration MO method),<sup>7</sup> EHT (extended Hückel type),<sup>9</sup> and an ab initio method using contracted Gaussian functions.<sup>8</sup> Although there was a variation in orbital energies and their relative sequence, the methods were unanimous in predicting a ligand (allyl) orbital as the highest occupied MO (HOMO). Shortly thereafter, a He (I) photoelectron (PE) spectroscopic investigation of **1** arrived at the quite different ordering that the HOMO was mainly a metal 3d type with the  $\pi$ -ligand orbitals lying lower by about 1.3 eV.<sup>10</sup> This interpretation invoked Koopmans' theorem<sup>11</sup> which equates the vertical ionization energy (IE) with a negative SCF-orbital energy. Subsequently another ab initio calculation was published taking into account electron reorganization after ionization<sup>12</sup> which is neglected in the

Koopmans approximation.<sup>11,13</sup> Ionization energies stemming from mainly d orbitals were found to be stabilized by reorganization vastly more than those corresponding to ligand ionization. This implied that the HOMO was mainly a ligand type although the first ionization energy referred to a metal d orbital—i.e., Koopmans' theorem fails for **1**. Although there had been earlier examples of this failure,<sup>13-15</sup> they applied to smaller differences in energy and were not nearly so dramatic as in this case. The PE spectral interpretation was now, however, in substantial agreement with the most extensive calculation done on such a molecule. Since that time, bis( $\pi$ -allyl)nickel has become an oft quoted example for the large scale failure of Koopmans' theorem.<sup>16</sup> However, some skepticism has remained and Fenske for instance has suggested further examination of this system.<sup>17</sup>

During the course of an investigation of methyl substituent effects on **1** as studied by PES, we began to question this seemingly settled question. In this paper we present evidence which supports an ordering more consistent with the earlier MO results and hence a nearer validity of Koopmans' theorem. It is also of some interest to examine the effect of subtle changes in a ligand upon the overall electronic levels since ligand change is of profound influence on the catalytic activity of a given metal atom. Bis( $\pi$ -allyl)nickel is a reasonable choice here also because of the catalytic activity of nickel complexes